Computation of Gravity Gradients Over Europe For Calibration/Validation of GOCE Data [†]

H. Denker
Institut für Erdmessung, Universität Hannover, Schneiderberg 50, D-30167 Hannover, Germany
E-mail: denker@ife.uni-hannover.de; Fax: +49-511-7624006

Abstract. The upcoming GOCE satellite mission is expected to map the Earth's gravity field with unprecedented accuracy. Besides the instrument calibrations on the ground and in orbit, there is a need to check the calibration throughout the two measurement phases without direct interference with the satellite operation. One promising method for the validation and calibration of GOCE data is the use of ground gravity data from some well-surveyed areas, upward continued to satellite altitude.

The least squares spectral combination technique is applied to the computation of gravity gradients in space. The necessary methodology is developed, and an error analysis is performed considering the errors in the terrestrial gravity data and the global geopotential model. The results show that accuracies at the level of a few mE (1 mE = 10^{-3} E, 1 E = 10^{-9} s^{-2}) are possible. The practical computations are based on the gravity and terrain data collected within the framework of the European Geoid Project. The contribution of each of the data sets involved in the combination process (gravity, terrain, global model) is discussed. Further numerical studies are presented regarding the effect of the satellite altitude, the resolution of the input data, the integration radius, the global geopotential model employed, and the use of terrain data. The results suggest the use of a high-degree global model, terrain information to avoid aliasing effects, a data resolution of 5′ to 10′, and a sufficiently large integration radius ($\geq 5°$) for accuracies of a few mE.

Keywords. Satellite gradiometry, GOCE mission, gravity gradients, validation, calibration

1 Introduction

The GOCE gravity field mission aims at providing an improved global geoid with an accuracy of 0.01 m at a spatial resolution of about 100 km, and a corresponding gravity accuracy of 1 mgal (ESA, 1999). For this purpose, a three-axis gravity gradiometer and high-low satellite-to-satellite-tracking from GPS satellites are combined to derive the gravity field information. Due to limitations in the performance of the accelerometers, the envisaged gradiometer accuracy of 4 mE/√Hz is limited to the measurement bandwidth of 5 to 100 mHz. Besides the instrument calibrations on the ground and in orbit, there is a need to check the calibration throughout the two measurement phases without direct interference with the satellite operation. One promising method for the validation and calibration of GOCE data is the use of ground gravity data from some well-surveyed areas, upward continued to satellite altitude (e.g., Arabelos and Tscherning, 1998).

This contribution focuses on the computation of the vertical gravity gradients. The calibration of the GOCE data itself is not discussed here. The methodology used is described in Section 2, which is based on the least squares spectral combination technique in conjunction with a remove-restore procedure. An error study is provided in Section 3, considering the errors in the terrestrial data and the global geopotential model. The truncation error, resulting from a limited integration in a local cap, is also discussed. In Section 4, the numerical experiments are described. They are based on gravity and terrain data collected within the framework of the European Geoid Project. The numerical studies are concerned with the contribution of the individual data sets to the final solution, the input data resolution, as well as the effect of the satellite altitude, the terrain data, and the global geopotential model.

2 Methodology

The least squares spectral combination technique (Wenzel, 1981; Sjöberg, 1980) is used for the computation of gravity gradients at satellite altitude. For the Earth's disturbing potential, T, the spherical harmonic series representation is adopted in the form

$$T = \frac{GM}{r} \sum_{l=2}^{\infty} \left(\frac{a}{r}\right)^l \sum_{m=0}^{l} \left(\overline{\Delta C}_{lm} \cos m\lambda + \overline{\Delta S}_{lm} \sin m\lambda\right) \overline{P}_{lm}(\cos\theta),$$

$$(1)$$

where (θ, λ, r) are the spherical coordinates (polar distance, longitude, radius), GM is the geocentric gravitational constant, a is the semi-major axis of

the reference ellipsoid, $\overline{\Delta C}_{lm}$, $\overline{\Delta S}_{lm}$ are the fully normalized potential coefficients, $\overline{P}_{lm}(\cos\theta)$ are the fully normalized associated Legendre functions, and l,m are the degree and order of the expansion. Equation (1) can be re-written by introducing a mean Earth radius R and the disturbing potential surface harmonics T_l (referring to R):

$$T = \sum_{l=2}^{\infty}\left(\frac{R}{r}\right)^{l+1}T_l , \qquad (2)$$

$$T_l = \frac{GM}{R}\left(\frac{a}{R}\right)^l\sum_{m=0}^{l}\left(\overline{\Delta C}_{lm}\cos m\lambda + \overline{\Delta S}_{lm}\sin m\lambda\right)\overline{P}_{lm}(\cos\theta). \qquad (3)$$

The gravity anomalies, serving as the primary input data in this study, are related to the disturbing potential T by the fundamental equation of physical geodesy. In a spherical approximation, this reads

$$\Delta g = -\frac{\partial T}{\partial r} - \frac{2}{r}T = \sum_{l=2}^{\infty}\left(\frac{R}{r}\right)^{l+2}\frac{l-1}{R}T_l = \sum_{l=2}^{\infty}\left(\frac{R}{r}\right)^{l+2}\Delta g_l , \quad (4)$$

where Δg_l are the gravity anomaly surface harmonics. Equation (4) can be inverted using the orthogonality relations and a constant radius ($r{=}R$) approximation, yielding

$$T_l = \frac{R}{l-1}\Delta g_l = \frac{R}{4\pi}\frac{2l+1}{l-1}\iint_{\sigma}\Delta g\,P_l(\cos\psi)d\sigma . \qquad (5)$$

From Eq. (5), Stokes's formula can be derived by summing up all surface harmonics T_l for degrees 2 to ∞ and by subsequent division with normal gravity γ (i.e., Bruns's formula).

There is now the possibility to derive the surface harmonics of the disturbing potential from two different data sources, namely from the coefficients of a global geopotential model via Eq. (3), and from gravity anomalies via Eq. (5). In the spectral combination technique, both quantities are combined using spectral weights w_l, depending on the degree l. After introducing the indexes M for the global model and G for the terrestrial gravity anomaly component, the combination solution for the disturbing potential surface harmonic can be written as

$$\hat{T}_l = w_l^M T_l^M + w_l^G T_l^G . \qquad (6)$$

The spectral weights for the two input data sets can be determined empirically, e.g., by filters suggested in Haagmans et al. (2002), or by least squares adjustment or collocation techniques, which take into account the given error estimates of the spectral components T_l^M and T_l^G. For the least squares adjustment solution, the spectral weights for the

gravity anomaly component are obtained by

$$w_l^G = w_l = \frac{\sigma_l^2(\varepsilon_{T^M})}{\sigma_l^2(\varepsilon_{T^M}) + \sigma_l^2(\varepsilon_{T^G})} , \qquad (7)$$

where $\sigma_l^2(\varepsilon_{T^M})$ and $\sigma_l^2(\varepsilon_{T^G})$ are the error degree variances for the geopotential model and the terrestrial gravity data, respectively, which can be derived from the potential coefficient standard deviations and an error covariance function of the gravity data (for details see, e.g., Wenzel 1982).

The sum of the spectral weights is expressed by

$$s_l = w_l^M + w_l^G , \qquad (8)$$

yielding $s_l = 1.0$ for the empirically determined weights and for the least squares adjustment solution, and $s_l \leq 1.0$ for the collocation solution due to the smoothing property inherent in this method.

Combining Eqs. (6) and (8) in the form $w_l^M = s_l - w_l^G$, while dropping the index G, gives the following result for the combined disturbing potential surface harmonics:

$$\hat{T}_l = s_l T_l^M + w_l(T_l^G - T_l^M) = \hat{T}_l^M + \hat{T}_l^G . \qquad (9)$$

The major advantage of rewriting the surface harmonic terms in the above equation is, that this basically results in a remove-restore procedure, i.e. the first part of Eq. (9) is the usual geopotential model component (for $s_l = 1.0$), and the second part contains the difference between the terrestrial gravity anomaly and the global model component. This yields significant advantages in the numerical evaluation, because the difference terms average out at larger distances (see also below). Summing all combined surface harmonics $\hat{T}_l$ according to Eq. (2) for degrees 2 to ∞ yields the final disturbing potential $\hat{T} = \hat{T}^M + \hat{T}^G$. However, as this study is primarily dealing with the computation of gravity gradients, and due to space restrictions, the complete formulas for $\hat{T}$ are not presented here.

The gravity gradients, i.e. the second derivatives of T, are derived in a (x,y,z) local spherical Cartesian coordinate system (north, east, radial). All six gravity gradients (T_{xx}, T_{xy}, T_{xz}, T_{yy}, T_{yz}, T_{zz}) are needed in order to be able to compute the gravity gradients in any rotated coordinate system by the equation $\mathbf{T_{ij}^R = R\,T_{ij}\,R^T}$, where $\mathbf{R}$ is the rotation matrix. In this study, however, the investigations are restricted to the radial (vertical) gravity gradients

$$T_{zz} = T_{rr} = \frac{\partial^2 T}{\partial r^2} , \qquad (10)$$

as this is the most dominant and important component. Applying Eq. (10) to the combined disturbing

potential $\hat{T}$ yields

$$\hat{T}_{rr} = \sum_{l=2}^{\infty} \left(\frac{R}{r}\right)^{l+3} \frac{(l+1)(l+2)}{R^2} \hat{T}_l = \sum_{l=2}^{\infty} \left(\frac{R}{r}\right)^{l+3} \hat{T}_{rr_l} = \hat{T}_{rr}^M + \hat{T}_{rr}^G ,$$
(11)

with the usual vertical gravity gradient from the global geopotential model (for $s_l = 1.0$)

$$\hat{T}_{rr}^M = \frac{GM}{r^3} \sum_{l=2}^{l_{max}} \left(\frac{a}{r}\right)^l (l+1)(l+2)s_l$$
$$\times \sum_{m=0}^{l} \left(\overline{\Delta C_{lm}} \cos m\lambda + \overline{\Delta S_{lm}} \sin m\lambda\right) \overline{P_{lm}}(\cos\theta),$$
(12)

and the gravity anomaly contribution

$$\hat{T}_{rr}^G = \frac{R}{4\pi} \iint_{\sigma} (\Delta g - \Delta g^M) W_{rr}(\psi, r) d\sigma ,$$
(13)

with the integration kernel

$$W_{rr}(\psi, r) = \sum_{l=2}^{\infty} \left(\frac{R}{r}\right)^{l+3} \frac{(l+1)(l+2)}{R^2} \frac{2l+1}{l-1} w_l P_l(\cos\psi) ,$$
(14)

where r is now the computation radius for the gradients (i.e., the radius to satellite altitude), and ψ is the spherical distance. Again, a constant radius approximation is used. From Eq. (13), the effect of rearranging the terms according to Eq. (9) becomes clear, resulting in a remove-restore procedure, which can also be extended to the inclusion of terrain effects. The major advantage is, that $\Delta g - \Delta g^M$ in Eq. (13) is a small quantity that averages out at larger distances, allowing the truncation of the integration to a local cap. Furthermore, if the gravity anomalies Δg^M in Eq. (13) are computed from a high-degree global geopotential model in an exact way or using ellipsoidal approximations, the use of spherical and constant radius approximations for the residual quantities in Eqs. (11) to (14) is clearly justified.

3 Accuracy Estimation

In this Section, error estimates for the gravity gradients are provided. The computations are based on Eqs. (11) to (14) and take into account the errors in the terrestrial gravity data and the global model. Furthermore, the truncation error, resulting from a limited integration of Eq. (13) out to a spherical distance ψ_{max} only, is discussed. In this study, three different sets of spectral weights and their corresponding integral kernels are considered (Fig. 1).

The first set of spectral weights (case A) is identical with the data set used to develop the EGG97 geoid model (Denker and Torge, 1998). It is based on the EGM96 coefficient errors, a 2 mgal standard deviation (std.dev.) of the gravity anomalies, and a simple distance-dependent correlation model in the form $r(\psi) = \exp(-4\psi [°])$. The spectral weights were derived from a least squares adjustment solution according to Eq. (7). The 2 mgal std.dev. for the terrestrial data was chosen from extensive tests in order to retain at least the longest wavelengths of the EGM96 model in the combination solution, which was not the case with a 1 mgal std.dev. The second set of spectral weights (case B) uses the EIGEN-1S coefficient standard deviations (Rev. 1 error estimates, Reigber et al., 2002) and, in this case, a 1 mgal standard deviation for the gravity anomalies, with the same correlation model as above. The weights were again derived by the least squares adjustment technique. On the other hand, the weights for case C are based solely on empirical estimates, using a cosine-taper function between degrees 40 and 50.

The truncation error for the three integral kernels described above was derived using the frequency transfer function introduced by Wenzel (1982). Due to space restrictions, the formulas are not pre-
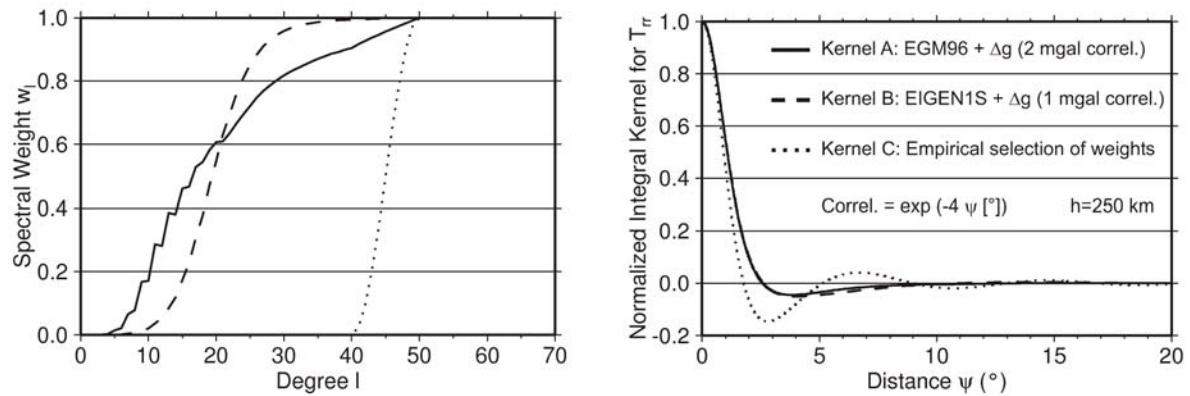

Fig. 1. Spectral weights (left) and corresponding integral kernels for T_{rr} (right) for cases A,B,C.

Table 1. RMS signal and error estimates for T_{rr} at 250 km satellite altitude. Units are mE.

Degree Range	EGM96 Signal	EGM96 Error	Spectral Combination Kernel A EGM96 + Correlated Δg		Spectral Combination Kernel A EGM96 + Uncorrelated Δg	
			$\sigma_{\Delta g} = 1$ mgal	$\sigma_{\Delta g} = 1/4$ mgal	$\sigma_{\Delta g} = 1$ mgal	$\sigma_{\Delta g} = 1/4$ mgal
2-18	184.2	1.3	0.8	0.7	0.8	0.7
19-36	115.7	5.8	1.7	1.2	1.6	1.2
37-50	88.4	8.7	1.4	0.6	1.1	0.6
51-90	90.4	13.9	1.5	0.4	1.0	0.3
91-180	31.5	7.9	0.6	0.2	0.4	0.1
181-360	1.4	0.6	0.0	0.0	0.0	0.0
> 360	-	-	0.0	0.0	0.0	0.0
2-∞	253.6	19.1	2.8	1.6	2.4	1.6
			1.7 *	0.4 *	1.1 *	0.3 *

* perfect global model up to degree 50

sented here, but only some numerical results are given. The RMS truncation error significantly depends on the maximum degree of the global model used. If EGM96 is used up to degrees 36, 180 and 360, respectively, the RMS truncation error for kernel A is 11.4, 2.5 and 2.1 mE for a truncation radius of $\psi_{max}=5°$, while these values reduce to 3.2, 0.5 and 0.4 mE for $\psi_{max}=10°$, and to 0.8, 0.1 and 0.1 mE for $\psi_{max}=15°$. Corresponding results are available for cases B and C. Thus, with a sufficiently large integration radius, the truncation errors can be kept well below the 1 mE level.

Based on Eqs. (9) and (11), the error estimates for the computed gravity gradients can be derived by straightforward error propagation. The error covariance function is given by

$$Cov(\varepsilon_{\hat{T}_{rr}}, \varepsilon_{\hat{T}_{rr}}, \psi) = \sum_{l=2}^{\infty} \left(\frac{R^2}{rr'}\right)^{l+3} \left(\frac{(l+1)(l+2)}{R^2}\right)^2 \sigma_l^2(\varepsilon_{\hat{T}}) P_l(\cos\psi),$$
(15)

with the error degree variances of the combined disturbing potential

$$\sigma_l^2(\varepsilon_{\hat{T}}) = \begin{cases} (s_l - w_l)^2 \sigma_l^2(\varepsilon_{T^M}) + w_l^2 \sigma_l^2(\varepsilon_{T^G}) & \text{for } l \leq l_{max} \\ \sigma_l^2(\varepsilon_{T^G}) & \text{for } l > l_{max} \end{cases}.$$
(16)

Table 1 shows the signal and error components for the T_{rr} gradients, based on EGM96, as well as the error estimates based on the spectral combination technique (i.e., combining EGM96 and the terrestrial gravity data using kernel A). For the latter case, error estimates are provided for correlated (see above) and uncorrelated gravity anomaly errors; the assumed anomaly accuracy is 1 or 0.25 mgal. The total error (bottom line in Table 1) and the contributions from different spectral bands are provided. All values in Table 1 refer to a satellite

altitude of 250 km. The EGM96 signal is about 250 mE with an error estimate of about 20 mE. For the spectral combination solutions, the error estimates from the correlated and uncorrelated input gravity data do not differ very much. For a 1 mgal accuracy of the gravity data, the total error is 2.8 mE and 2.4 mE for the correlated and uncorrelated gravity data, respectively. In both cases, the major error contribution comes from degrees less than 50. However, this situation will improve with the CHAMP and GRACE missions, and therefore the total error is also given for a global model perfect up to degree 50 (values are marked by an asterisk). For a more optimistic scenario with a 0.25 mgal anomaly accuracy, the total accuracy is 1.6 mE for both the correlated and uncorrelated case, with the dominant contributions again coming from the errors of the global model (below degree 50). Thus, sub-mE accuracies are only possible with significantly improved global Earth models and very accurate terrestrial data. From Table 1 it is also evident that the gradient signal above degree 180 is quite weak, which makes the recovery of such terms difficult.

4 Numerical Experiments

The numerical results presented in this Section are based on the terrestrial gravity and terrain data collected within the framework of the European Geoid Project (Denker and Torge, 1998). However, for this study, the detailed grids were merged to 5′×5′ grids. The combination of the terrestrial gravity and terrain data with a global geopotential model is based on the spectral combination technique in connection with a remove-restore procedure as described in Section 2. The integral formulas were evaluated by 1D FFT techniques. EGM96 is used to
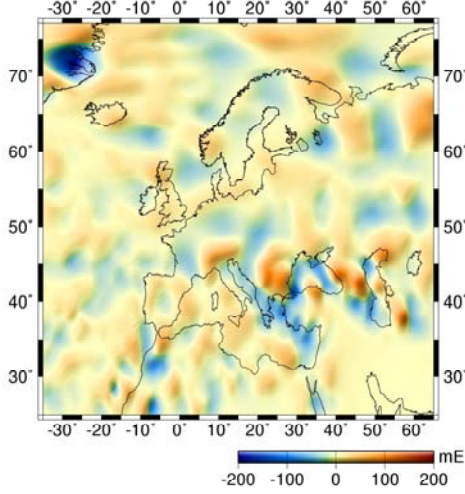
Fig. 2. Residual gravity gradients T'_{zz} at 250 km satellite altitude, computed from the terrestrial gravity data. Units are mE.
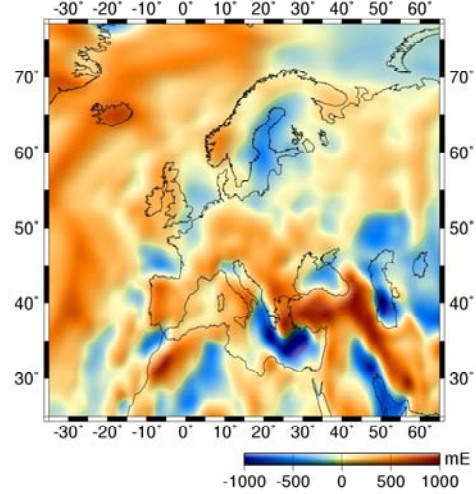
Fig. 3. Final gravity gradients $T_{zz} = T'_{zz} + T^M_{zz} + T^T_{zz}$ at 250 km satellite altitude. Units are mE.

provide the long wavelength gravity field components, while the topography is taken into account using the residual terrain model (RTM) reduction procedure with a 15′ moving average filter for the construction of the reference topography.

Table 2 shows the statistics of the relevant gravity field parameters, where the superscript M stands for the global model, and T stands for the topographic component. All gravity gradient computations refer to a satellite altitude of 250 km. The RMS of the residual gravity anomalies is 11.6 mgal. The direct vertical gravity gradient contribution from the terrain is very small due to the RTM method (0.6 mE RMS, 4.3 mE max.), while the contribution from the terrestrial gravity data is 23.7 mE RMS (about 200 mE max.), and the largest contribution comes from the global model (about 300 mE RMS and 1.5 E max.). Figures 2 and 3 show the contribution of the terrestrial gravity data and the final vertical gravity gradients over Europe.

The effect of the satellite altitude on the results was studied by repeating the above calculations for

a satellite altitude of 260 km, followed by differencing the 250 km and 260 km results. Table 3 shows the statistics of all relevant components. Again, the largest contribution to the differences is coming from the global model (15.4 mE RMS), while the corresponding value for the terrestrial gravity data is only 1.9 mE RMS.

Further studies were performed regarding the input grid size. For this purpose, the 5′×5′ grids were averaged to coarser grids, and then the gravity gradients were re-computed again, followed by an interpolation to the nodes of the detailed grid and a

Table 3. Statistics of the differences between gravity field components computed at 250 km and 260 km satellite altitude. Units are mE.

Parameter	Mean	RMS	Min.	Max.
$\delta T'_{zz}$	0.0	1.9	-16.5	13.9
δT^M_{zz} (EGM96)	1.2	15.4	-105.2	79.9
δT^T_{zz} (RTM)	0.0	0.1	-0.5	0.6
δT_{zz}	1.2	15.6	-102.6	80.7

Table 2. Statistics of the gravity field components involved in the remove-restore procedure. The gravity gradient components refer to a satellite altitude of 250 km.

Parameter		Mean	Std.dev.	RMS	Min.	Max.
$\Delta g' = \Delta g - \Delta g^M - \Delta g^T$	[mgal]	0.25	11.60	11.60	-168.87	194.82
T'_{zz}	[mE]	0.0	23.7	23.7	-194.8	130.3
T^M_{zz} (EGM96)	[mE]	117.8	285.3	308.7	-1466.3	985.1
T^T_{zz} (RTM)	[mE]	0.0	0.6	0.6	-3.0	4.3
$T_{zz} = T'_{zz} + T^M_{zz} + T^T_{zz}$	[mE]	117.8	285.8	309.2	-1447.0	963.2

comparison. The differences exceeded about 1 mE RMS for grid sizes larger than 15′; in this case, however, the maximum differences reach 15 to 20 mE. Thus, a grid size of 5′ to 10′ is preferable for highest accuracies.

Furthermore, the contribution from different integration radii was studied, with the results being strongly dependent on the integration kernel used and the magnitude of the signal, which is passed through that kernel. For kernel A and EGM96 complete to degree 360, the contribution from the zones outside $\psi > 10°$ is less than 1 mE RMS (2 mE max.), while for kernel B and EIGEN-1S (Reigber et al., 2002) to degree 119, the corresponding values are 1.9 mE RMS (8 mE max.). Thus, the employment of a high-degree geopotential model is advantageous, and a sufficiently large integration radius is required to keep the truncation error below acceptable limits.

The use of terrain information is twofold. As was shown above, the direct effect is very small for the RTM method. Nevertheless, terrain data plays an important role in the process of gravity anomaly gridding. To study this effect, the 5′×5′ input gravity anomaly grid was re-computed by simple averaging of the anomalies without taking into account any terrain information. It is well known that such a procedure is significantly affected by aliasing errors and yields strongly biased results. This is especially valid in the mountains, as the observations are usually made along roads in valleys, and are thus not representative for the area. The anomaly differences between the two grids reach about 10 mgal RMS (max. > 200 mgal), which transforms into corresponding gradient differences of 43 mE RMS (max. 600 mE over the Alps). Thus, the results without considering any terrain information in the gravity gridding process render the technique completely useless in mountainous areas.

The use of the global geopotential model was the final topic that was investigated. As well as EGM96, EIGEN-1S was also tested. Since EIGEN-1S is a satellite-only model with full power only up to about degree 36, test solutions with the EIGEN-1S augmented by EGM96 above degree 36 were also computed. Comparison of the relevant gradient solutions again showed that it is advantageous to use a high-degree model, i.e. the EIGEN-1S + EGM96 results were superior to the pure EIGEN-1S results. One reason for this may be that approximation and linearization errors (constant radius approximation, etc.) are significantly reduced for a high-degree reference model. The RMS difference between the EGM96 and the EIGEN-1S +

EGM96 combined gravity gradients was 3.9 mE (15 mE max.), and the differences show purely long wavelength structures, as expected.

5 Conclusions

Vertical gravity gradients T_{rr} were computed over Europe based on the gravity and terrain data from the European Geoid Project. The spectral combination technique was applied. The integral formulas were evaluated by 1D FFT, which is an efficient tool for production work. The error studies show that accuracies at the few mE level are possible in areas with a good gravity coverage and accuracy. The numerical experiments suggest to use a data grid size at the 5′ to 10′ level, an integration radius larger than 5°, terrain reductions to avoid/reduce aliasing effects, and a high-degree geopotential model as a reference field to reduce linearization and approximation errors. Computation of the full gravity gradient tensor is planned for the future.

References

Arabelos, D., C.C. Tscherning (1998). Calibration of satellite gradiometer data aided by ground gravity data. Journal of Geodesy, 72:617-625.

Denker, H., W. Torge (1998). The European gravimetric quasigeoid EGG97 – An IAG supported continental enterprise. In: R. Forsberg et al. (eds.), Geodesy on the Move – Gravity, Geoid, Geodynamics, and Antarctica, *IAG Symp. Proceed., Springer Verlag, Berlin, Heidelberg*, 119:249-254.

ESA (1999). Gravity field and steady-state ocean circulation mission. Reports for Mission Selection, The Four Candidate Earth Explorer Core Missions, ESA SP-1233(1).

Haagmans, R., K. Prijatna, O. Omang (2002). An alternative concept for validation of GOCE gradiometry results based on regional gravity. Proceed. Gravity and Geoid 2002, GG2002, August 26-30, 2002, Thessaloniki, this volume.

Reigber, Ch., G. Balmino, P. Schwintzer, R. Biancale, A. Bode, J.-M. Lemoine, R. Koenig, S. Loyer, H. Neumayer, J.-C. Marty, F. Barthelmes, F. Perosanz, S.Y. Zhu (2002). A high quality global gravity field model from CHAMP GPS tracking data and accelerometry, *Geophysical Research Letters, Vol. 29, No. 14*, doi:10.1029/2002GL015064.

Sjöberg, L. (1980). Least squares spectral combination of satellite and terrestrial data in physical geodesy. Internat. Symp. on Space Geodesy and Its Application, Cannes, 1980, *Annales de Géophysique*, 37:25-30.

Wenzel, H.G. (1981). Zur Geoidbestimmung durch Kombination von Schwereanomalien und einem Kugelfunktionsmodell mit Hilfe von Integralformeln. *Zeitschr. f. Verm.wesen*, 106:102-111.

Wenzel, H.G. (1982). Geoid computation by least squares spectral combination using integral formulas. *Proceed. of the General Meeting of the IAG, Tokyo, May 7-15*, 438-453.